Structural studies of secondary crystallization products of the $Fe_{23}B_6$-type in a nanocrystalline FeCoB-based alloy

Jianguo Long,[a] P. R. Ohodnicki, D. E. Laughlin, and M. E. McHenry
Materials Science and Engineering, Carnegie Mellon University, Pittsburgh, Pennsylvania 15213

T. Ohkubo and K. Hono
National Institute for Materials Science, Tsukuba 305-0047, Japan

(Presented on 11 January 2007; received 31 October 2006; accepted 7 February 2007; published online 8 May 2007)

A stable $Fe_{23}B_6$-type phase formed in a nanocomposite soft magnetic alloy $Fe_{40}Co_{40}Nb_4B_{13}Ge_2Cu_1$ after thermal treatment was investigated. The primary crystallization temperature and second crystallization temperature for this alloy were determined to be 405 and 740 °C, respectively. After annealing the sample at 820 °C for 1 h, a $Fe_{23}B_6$-type phase $(FeCoNb)_{23}B_6$ was observed. The structural information was investigated by x-ray diffraction, transmission electron microscopy, and three-dimensional atom probe. The $Fe_{23}B_6$-type phase contains about 33±5 at. % Fe, 38±5 at. % Co, 7±1 at. % Nb, and 20±3 at. % B. The Nb atoms tend to occupy the 8*c* sites and Co/Fe atoms occupy the 4*a*, 32*f*, and 48*h* sites of the *Fm*3*m* space group for this structure. © *2007 American Institute of Physics*. [DOI: 10.1063/1.2714250]

INTRODUCTION

Fe-based nanocrystalline soft magnetic alloys are promising candidate materials for power conversion applications due to their excellent soft magnetic properties and low losses at high frequencies. Nanocomposite magnetic materials are synthesized by the partial crystallization of an amorphous alloy precursor. Current state of the art nanocomposite soft magnetic alloys consist of nanometer size α-FeSi (DO3) (FineMet),[1] α-Fe (bcc) (NANOPERM),[2] and α'-FeCo (B2) (HITPERM) (Ref. 3) grains dispersed in a residual amorphous matrix. When these nanocomposite soft magnetic materials are crystallized above their secondary crystallization temperature, the residual amorphous phase forms FeB-, Fe_2B-, Fe_3B-, or even $Fe_{23}B_6$-type phases. Phases having a $TL_{23}M_6$ (such as $Fe_{23}B_6$ and $Fe_{23}C_6$),[4–7] $TL_{23}TE_6$ (such as $Fe_{23}Zr_6$), or $TL_{23}RE_6$ (such as $Fe_{23}Gd_6$) (Ref. 8) stoichiometry (where TL=late transition metal, *M*=Metalloid and TE=early transition metal, and RE=rare earth) are ubiquitous in important nanocomposite soft magnetic, martensitic, and rare earth-transition metal permanent magnet systems. It is therefore important to study the underlying structure and microstructure of these phases in order to understand the origin of important properties for technical applications of these materials. Here we focus on the $Fe_{23}B_6$ phase as a secondary crystallization product in nanocomposite soft magnet systems. The information and analysis reported here are also likely to be important for understanding other magnetic systems in which this phase is present.

The $Fe_{23}B_6$ phase adopts the $Cr_{23}C_6$ prototype structure with the *Fm*3*m* space group and Pearson symbol cF116. This phase is a metastable phase, which can easily decompose into Fe_3B and α-Fe in the Fe–B alloy systems.[4,9] However, when the Fe atom site is partially substituted for by another transition metal atom (such as Nb, Co, or Ni),[4–6] the phase is stabilized and more easily retained. Recently, it has been reported that this phase is observed as a secondary crystallization product of amorphous ribbon after precursors.[4–6,10,11]

In this work, we found that a stable $Fe_{23}B_6$-type phase precipitated as a secondary crystallization product in a $Fe_{40}Co_{40}Nb_4B_{13}Ge_2Cu_1$ soft magnetic alloy. X-ray diffraction (XRD), transmission electron microscopy (TEM), and atomic probe field ion microscopy (APFIM) were used to investigate the details of the structure of this phase.

EXPERIMENT

Amorphous ribbons, ~30 μm thick and ~3 mm wide, of nominal composition $Fe_{40}Co_{40}Nb_4B_{13}Ge_2Cu_1$ were prepared by single roller melt spinning. The alloy was induction melted in a quartz crucible and cast within an argon atmosphere onto a copper wheel rotating at ~50 m/s in a vacuum chamber. The amorphous samples were subsequently crystallized by sealing them in evacuated silica tubes, placing them in a preheated furnace at prescribed temperatures, and finally quenching them in water at room temperature.

X-ray diffraction (XRD) with Cu $K\alpha$ radiation was used to study the structure of the alloy in amorphous and annealed states. Thermomagnetic measurements were performed in a vibrating sample magnetometer (VSM) equipped with a vacuum furnace. Magnetization versus temperature data were collected in a VSM with an oven programed to ramp at 2 °C/min from 50 to 980 °C under a constant field intensity of 5 kOe. A JEOL JEM2000 transmission electron microscope operated at 200 keV was employed to characterize the microstructure. TEM samples were prepared by ion milling. An energy compensated three-dimensional atom probe (3DAP) was used in this study.

[a]Electronic mail: jianguol@andrew.cmu.edu

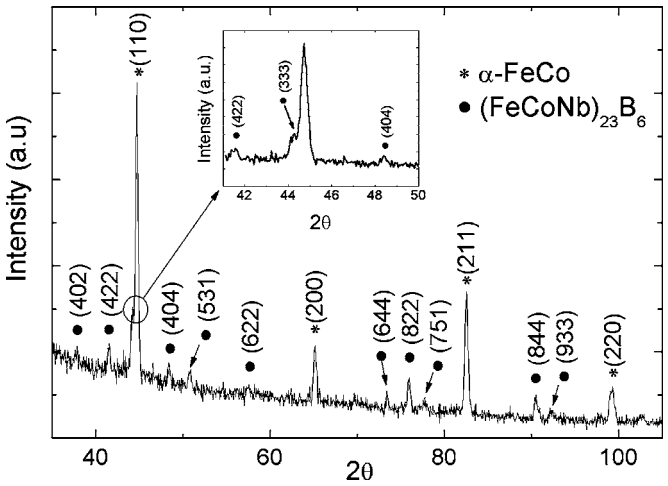

FIG. 1. XRD data for sample $Fe_{40}Co_{40}Nb_4B_{13}Ge_2Cu_1$ after being annealed at 820 °C for 1 h.

RESULTS AND DISCUSSION

The magnetization versus temperature curve for an amorphous sample heated from 50 to 980 °C at 2 °C/min heating rate under 5 KOe magnetic field was obtained by VSM in order to determine the crystallization temperature. The gradual decrease in magnetization from the initial state reflects the approach of the amorphous phase to its Curie temperature. A moment increase beginning at ~405 °C is a consequence of the primary crystallization in which a bcc-derivative Fe–Co is the product. Evidence for the second crystallization is observed at 740 °C, where there is again a small increase in magnetization. The α-γ first order transition is indicated by a sharp drop in the magnetization between 900 and 930 °C.

XRD verified that the sample was amorphous in the as-melt-spun state. Prior to annealing the sample at 820 °C secondary phases such as $(FeCoNb)_{23}B_6$ were observed in the sample. Figure 1 shows the XRD pattern for a sample after it was annealed at 820 °C for 1 h. Both the α-FeCo phase and $(FeCoNb)_{23}B_6$ phase were observed in the sample. Analysis of the XRD data shows the $(FeCoNb)_{23}B_6$ phase to have a lattice constant $a=10.63\pm0.01$ Å. A TEM microstructure and selected area diffraction pattern (SAD) are shown in Fig. 2. The grain size after annealing at 820 °C for 1 h is observed to be ~200 nm. The SADs show the presence of both α-FeCo and $(FeCoNb)_{23}B_6$ phases. A [321] zone electron diffraction pattern for the $(FeCoNb)_{23}B_6$ phase is shown in Fig. 2(b). The lattice constant for this $(FeCoNb)_{23}B_6$ phase determined from this SAD was 10.71 ± 0.05 Å, close to the value determined by XRD.

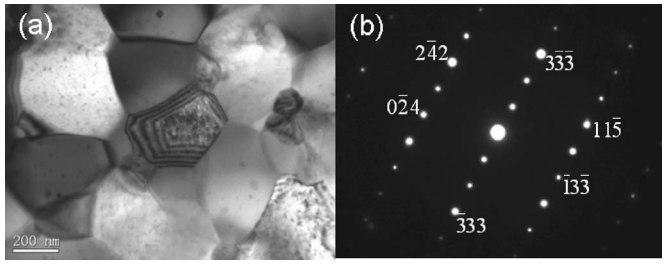

FIG. 2. (a) Bright field TEM image of sample $Fe_{40}Co_{40}Nb_4B_{13}Ge_2Cu_1$ after annealing at 820 °C for 1 h (b) Selected area diffraction pattern for a [321] zone axis of a $(FeCoNb)_{23}B_6$ particle.

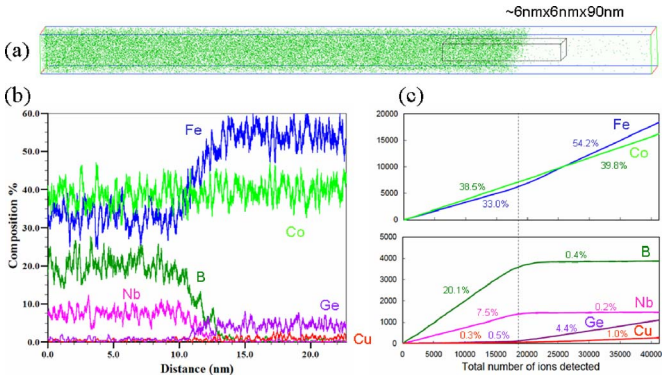

FIG. 3. (a) 3DAP elemental map and [(b) and (c)] concentration depth profiles obtained from a selected volume of $6\times6\times90$ nm^3.

The chemical partitioning of the alloying elements after crystallization is determined from 3DAP elemental mapping. Figure 3 shows the 3DAP analysis result for a $Fe_{40}Co_{40}Nb_4B_{13}Ge_2Cu_1$ alloy annealed at 820 °C for 1 h. Figure 3(a) shows the distribution of B in a volume of $6\times6\times90$ nm^3. To quantitatively evaluate the partitioning of the alloy elements, concentration depth profiles determined from the selected volume were obtained and are shown in Figs. 3(b) and 3(c). Figure 3(b) shows the α-FeCo grains to have an average composition: Fe 56 ± 5 at. %, Co 39 ± 5 at. %, and 4 ± 1 at. % Ge. Compared with the alloy without Ge atom, the Ge element present in FeCo grains decreases the α-γ transition temperature. Moreover, Cu is preferentially into α-FeCo grain because Cu provides the nucleation site during crystallization process. The $(FeCoNb)_{23}B_6$ phase in the alloy studied here is estimated to contain about 33 ± 5 at. % Fe, 38 ± 5 at. % Co, 7 ± 1 at. % Nb, and 20 ± 3 at. % B.

Table I summarizes the site occupation in the $Fe_{23}B_6$ structure and compares to the observed atomic concentration in this phase as determined from 3DAP data. In the $Fe_{23}B_6$ structure, B atoms occupy the 24*e* site of the *Fm*3*m* space group and Fe atoms occupy the 8*c*, 4*a*, 32*f*, and 48*h* sites. However, in our $Fe_{40}Co_{40}Nb_4B_{13}Ge_2Cu_1$ alloy, we conclude from APFIM data that the Fe sites in the $Fe_{23}B_6$ phase are partially substituted for by Co and Nb atoms. A comparison of the theoretical site concentration in unit cell and 3DAP data suggests that Nb atoms possibly occupy the 8*c* sites and Co atoms are randomly distributed on 4*a*, 32*f*, and 48*h* sites.

Large atoms, Nb and Co, cannot be incorporated inter-

TABLE I. $Fe_{23}B_6$ structure site occupancy.

Wyckoff class	Coordinates (x,y,z)	Sites in the unit cell (%)	3DAP data (at. %)
24*e*	(0.2764,0,0)	20.69%	B 20±3%
8*c*	(0.25,0.25,0.25)	7.00%	Nb 7±1%
4*a*	(0,0,0)	3.45%	Co 38±5%
32*f*	(0.3810,0.3810,0.3810)	27.59%	Fe 33±5%
48*h*	(0,0.1712,0.1712)	41.38%	

stitially nor can they substitute for boron. There are thus four plausible sites for these transition metal species, the iron sites of Wyckoff classes 4*a*, 8*c*, 32*f*, or 48*h*. The distances from 8*c* site to its nearest neighbor 32*f* and 48*h* sites are 0.2405 and 0.290 nm, respectively. It is therefore clear that the 8*c* site is a spacious site. When we compare the fraction of 8*c* sites in the $Fe_{23}B_6$ structure with the 3DAP observation of the content of Nb in $(FeCoNb)_{23}B_6$ phase, it can be seen that they closely match. Moreover, since Nb has a larger atomic radius than Fe or Co and the 8*c* site is a spacious site, it is likely that this is the site preferred by Nb. Therefore we postulate that Nb atoms occupy the 8*c* sites and Co/Fe atoms occupy 4*a*, 32*f*, and 48*h* sites of the $Cr_{23}C_6$ prototype structure. Recent band structure calculations[7] for the $Cr_{23}C_6$ phase have also shown the 8*c* sites to be preferred by atoms slightly larger than Fe, so replacement with Mo, Nb, Y, or Sc is postulated to stabilize this structure.

CONCLUSION

A metastable $Fe_{23}B_6$ phase was stabilized with Fe atom partially substituted by Co and Nb atoms in nanocomposite soft magnetic alloy $Fe_{40}Co_{40}Nb_4B_{13}Ge_2Cu_1$ after second crystallization. This stable $(FeCoNb)_{23}B_6$ phase, verified by XRD, TEM, and APFIM, has a lattice constant of 10.63 Å and Nb atoms tend to replace Fe atom at 8*c* sites.

ACKNOWLEDGMENTS

This work was supported by National Science Foundation DMR-0406220. The authors gratefully acknowledge useful discussions with Professor M. Widom of CMU.

[1] Y. Yoshizawa, S. Oguma, and K. Yamauchi, J. Appl. Phys. **64**, 6044 (1998).
[2] K. Suzuki, N. Ktaoka, A. Inoue, A. Makino, and T. Masumoto, Mater. Trans., JIM **31**, 743 (1990).
[3] M. A. Willard, D. E. Laughlin, M. E. McHenry, D. Thoma, K. Sickafus, J. O. Cross, and V. G. Harris, J. Appl. Phys. **84**, 6773 (1998).
[4] M. Imafuku, S. Sato, H. Koshiba, E. Matsubara, and A. Inoue, Scr. Mater. **44**, 2369 (2001).
[5] M. Shapaan, J. Gubicza, J. Lendvai, and L. K. Varga, Mater. Sci. Eng., A **375–377**, 785 (2004).
[6] B. Idzikowski and A. Szajek, Mater. Sci. **21**, 73 (2003).
[7] M. Widom and M. Mihalkovic, J. Mater. Res. **20**, 237 (2005).
[8] M. Zinkevich, N. Mattern, and I. Bacher, Z. Metallkd. **93**, 3 (2002).
[9] E. F. Kneller, IEEE Trans. Magn. **27** 3588 (1991).
[10] C.-Y. Um and M. E. McHenry, IEEE Trans. Magn. **40**, 2724 (2004).
[11] D. H. Ping, K. Hono, H. Kanekiyo, and S. Hirosawa, Acta Mater. **47**, 4641 (1999).